

Statistical Properties of a Cloud Ensemble: A Numerical Study

WEI-KUO TAO

General Sciences Corporation, Laurel, MD 20707

JOANNE SIMPSON

Laboratory for Atmospheres, NASA/Goddard Space Flight Center, Greenbelt, MD 20771

SU-TZAI SOONG

Department of Land, Air and Water Resources, University of California, Davis, CA 95616

(Manuscript received 30 December 1986, in final form 30 April 1987)

ABSTRACT

Two- and three-dimensional configurations of a cloud ensemble model are used to study the statistical properties of cloud ensembles under an observed large-scale condition. The basic design of the model has been presented in papers by Soong, Ogura, and Tao. An observed large-scale lifting and small amplitude random perturbations in the form of temperature fluctuations are imposed continuously in the model. The model then allows many clouds of different sizes to develop simultaneously. A 6-hour time integration is made to allow a large number of convective clouds to develop. After the model integration, horizontal and time averages of various relevant variables are computed to elucidate the statistical properties of clouds. The model is applied to the case of a well-organized intertropical convergence zone (ITCZ) rainband that occurred on 12 August 1974, during the Global Atmospheric Research Program's Atlantic Tropical Experiment.

The statistical properties of clouds, such as mass flux by cloud drafts and vertical velocity as well as condensation and evaporation associated with these cloud drafts are examined in this study. The cloud drafts are further subclassified as inactive and active. Separate contributions to cloud statistics in areas of different cloud activity are then evaluated. The model results compared well with those obtained from aircraft measurements. Some implications of model results to the cumulus parameterization problem are briefly discussed. A comparison between the two- and three-dimensional model simulations is also made.

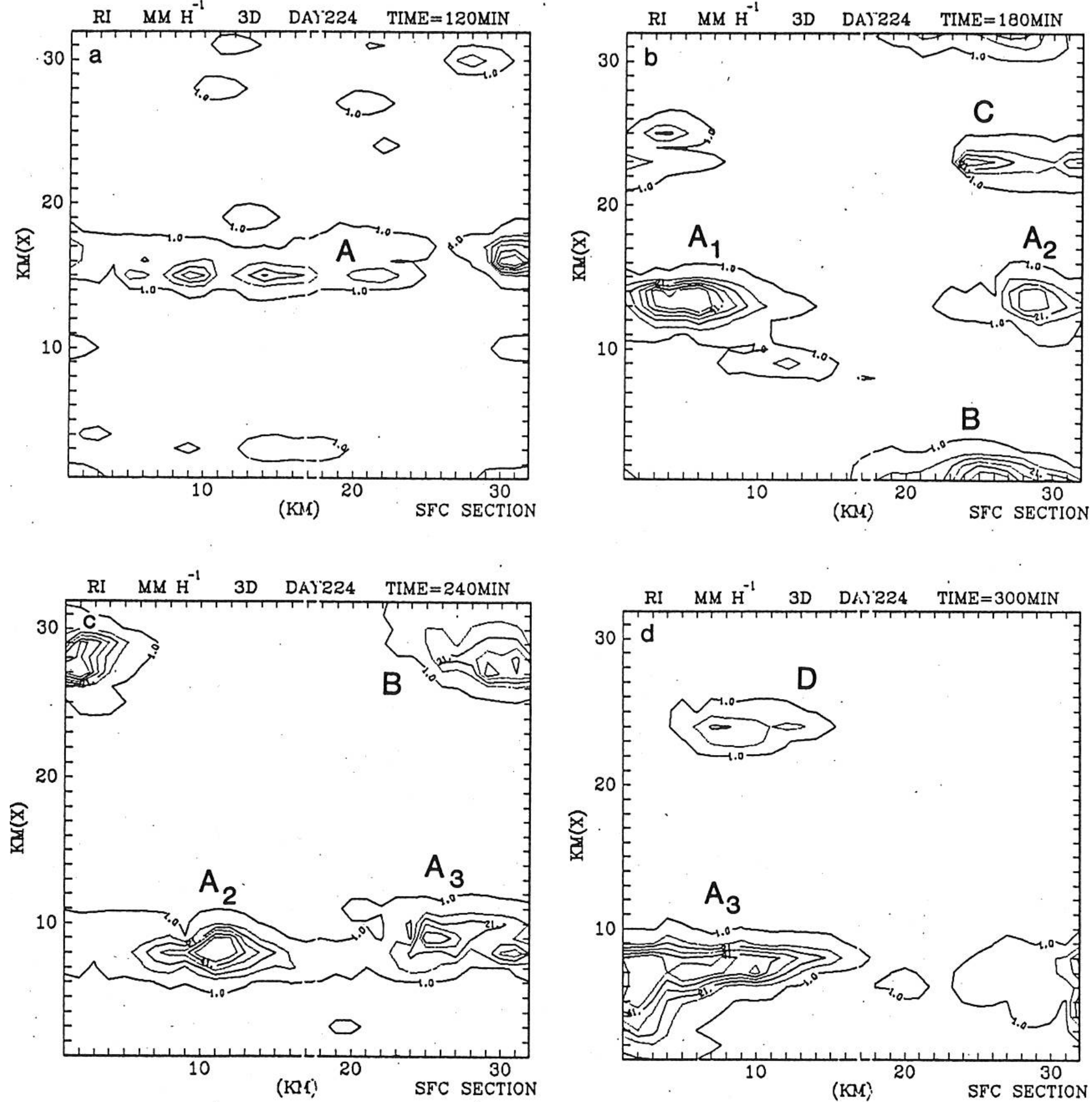
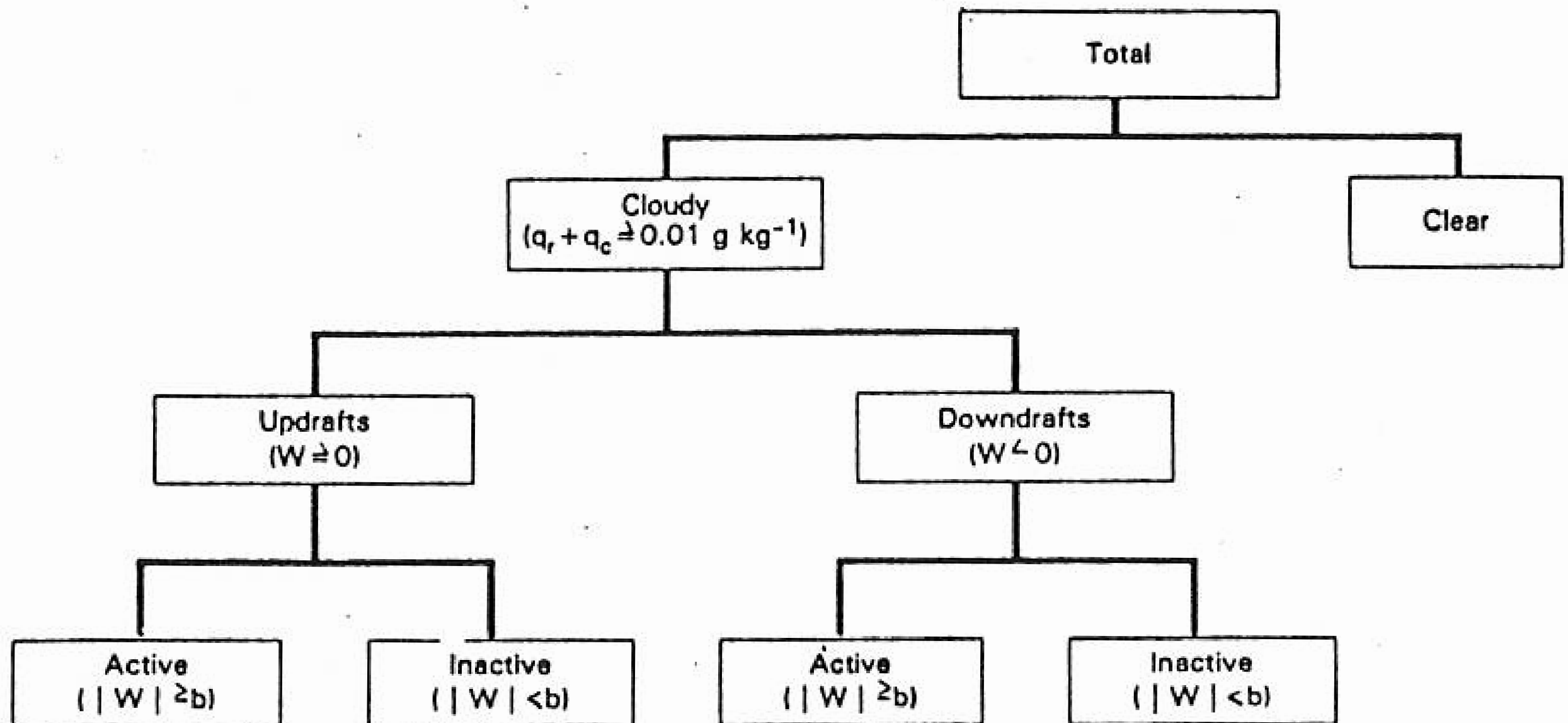


FIG. 1. Surface rainfall rate over the horizontal domain at (a) 120 min, (b) 180 min, (c) 240 min and (d) 300 min obtained from a three-dimensional simulation. The contour intervals are 10 mm h^{-1} starting at 1 mm h^{-1} .

TABLE 1. Calibration of clear, active and inactive cloud drafts.
 b is either 1 or 2 m s⁻¹.



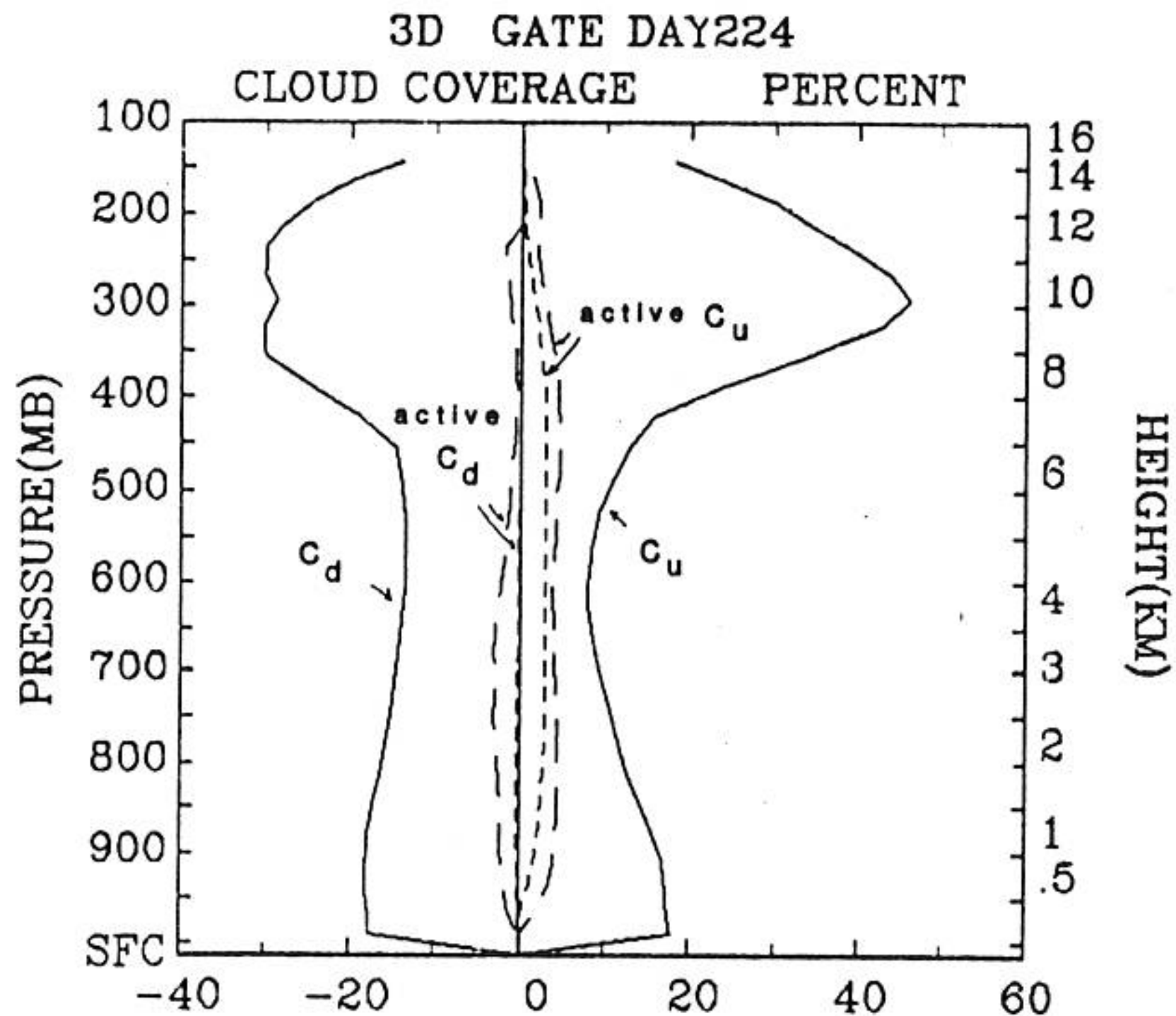


FIG. 2. Percent coverage of updraft and downdraft areas and active updraft and downdraft areas where the absolute vertical velocity exceeds 1 (long-dashed line) or 2 m s^{-1} (short-dashed line). The 2 m s^{-1} group is a subset of the 1 m s^{-1} group. C_u represents cloud updrafts and C_d represents cloud downdrafts. Time averages obtained from data at 1 min interval.

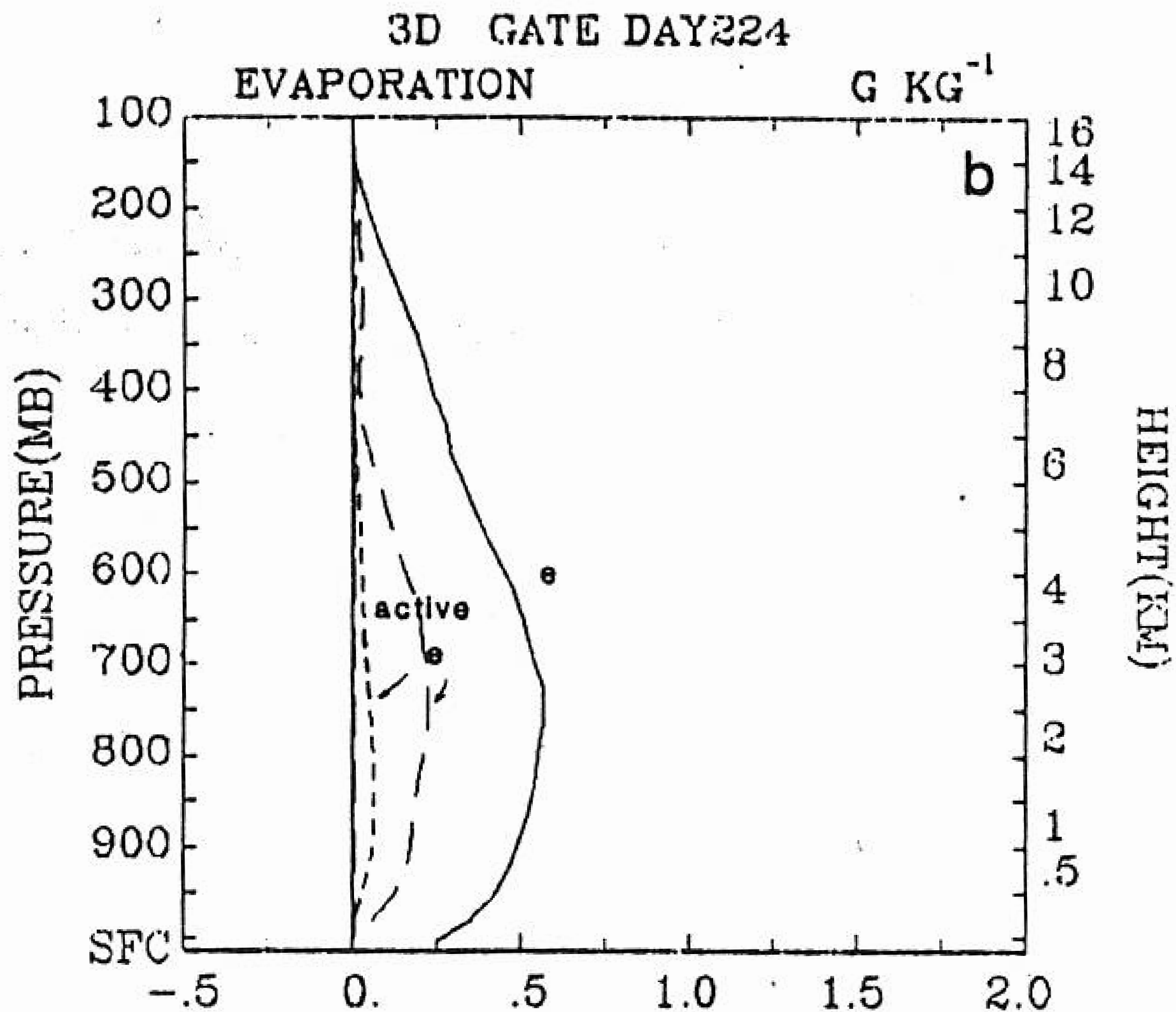
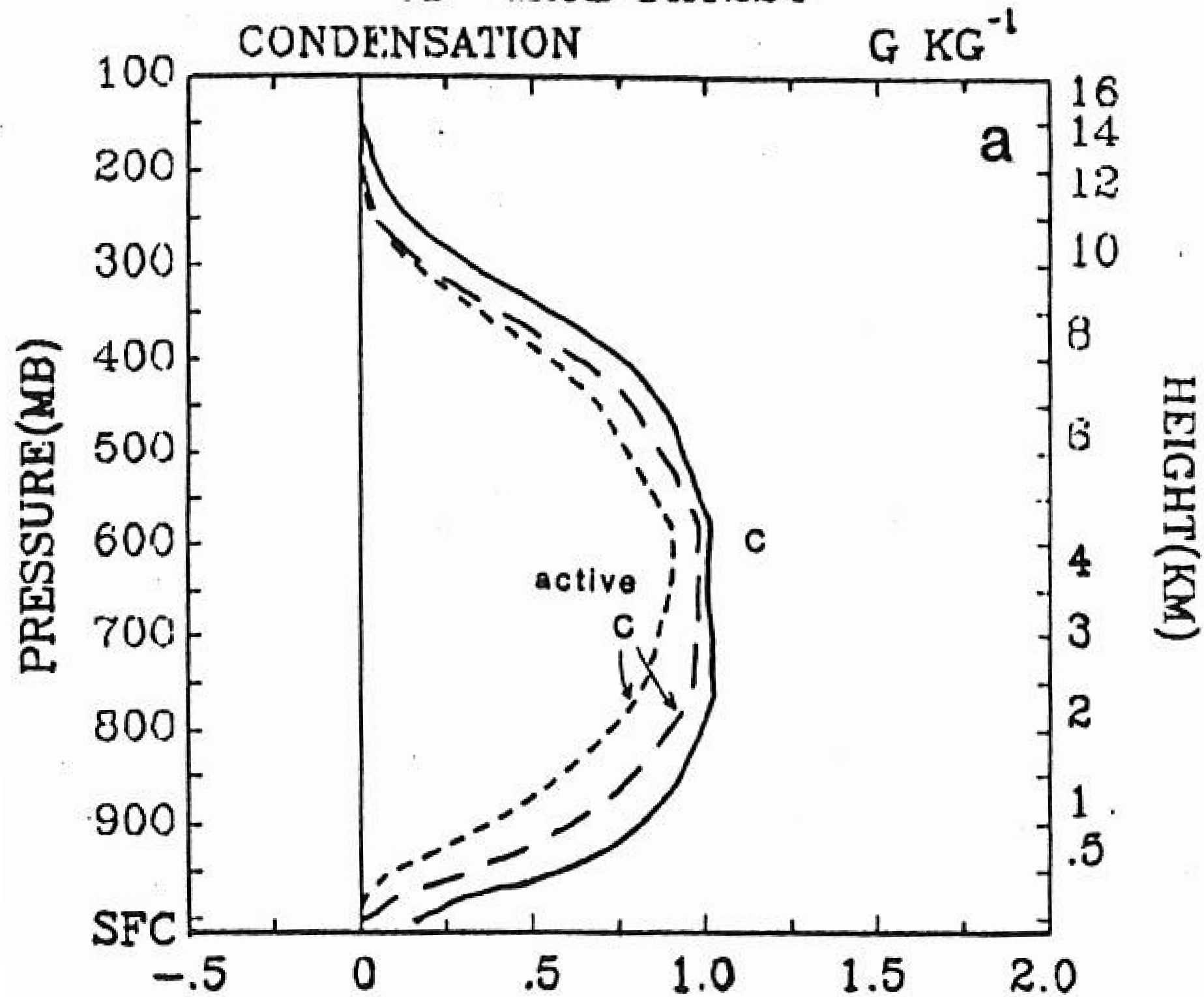


FIG. 4. (a) The vertical profile of condensation rates of updraft areas and active updraft areas where the absolute vertical velocity exceeds 1 or 2 m s^{-1} . (b) Same as a except for evaporation rates in cloud downdraft areas.

3D GATE DAY224



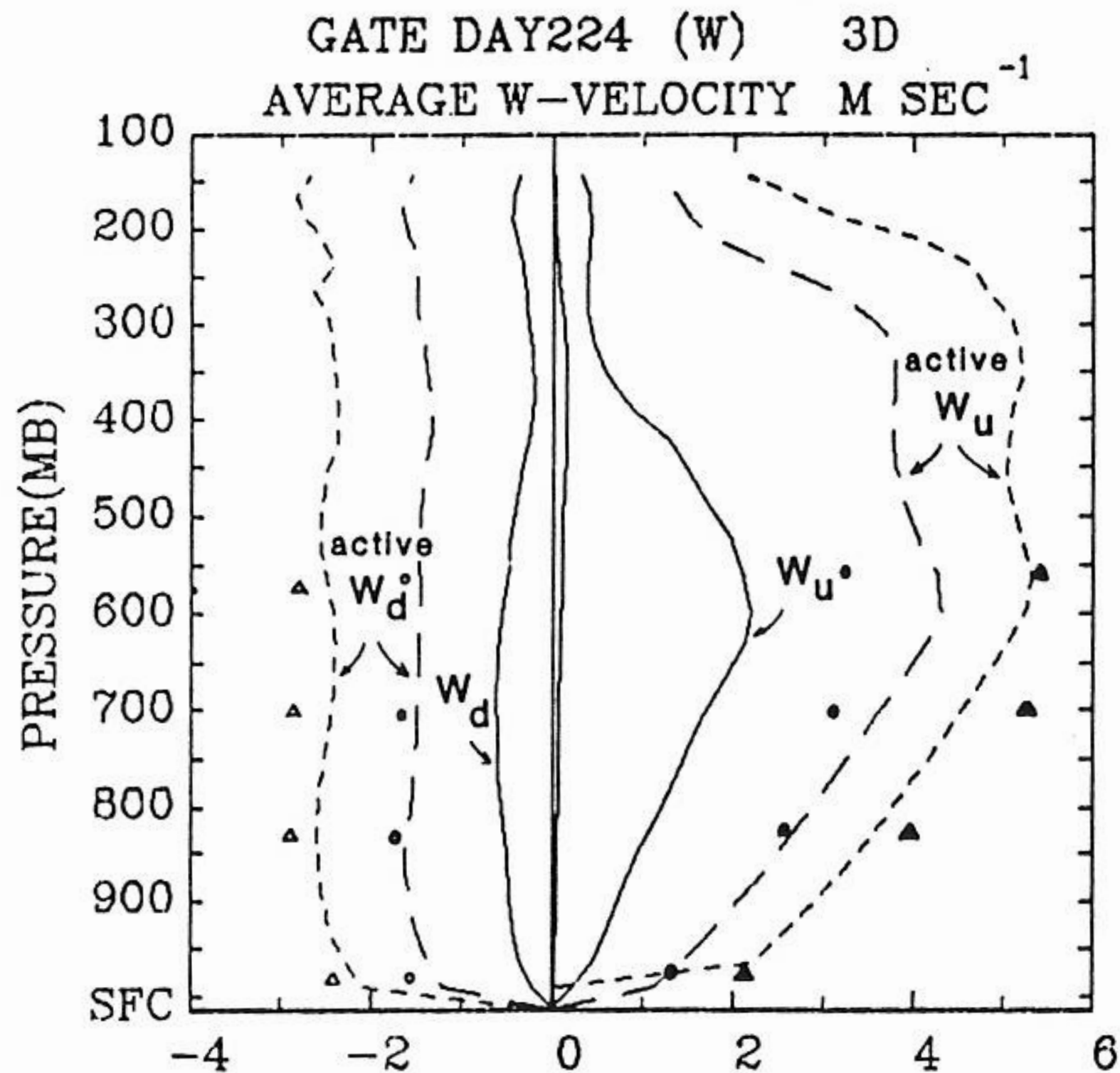


FIG. 8. The vertical profiles of the upward and downward mean velocities inside all clouds and the mean velocities inside the active updraft and downdraft areas. Aircraft measurements from Zipser and LeMone are also indicated by circles for the mean (50%) and by triangles for the strong (10%) intensity cores.

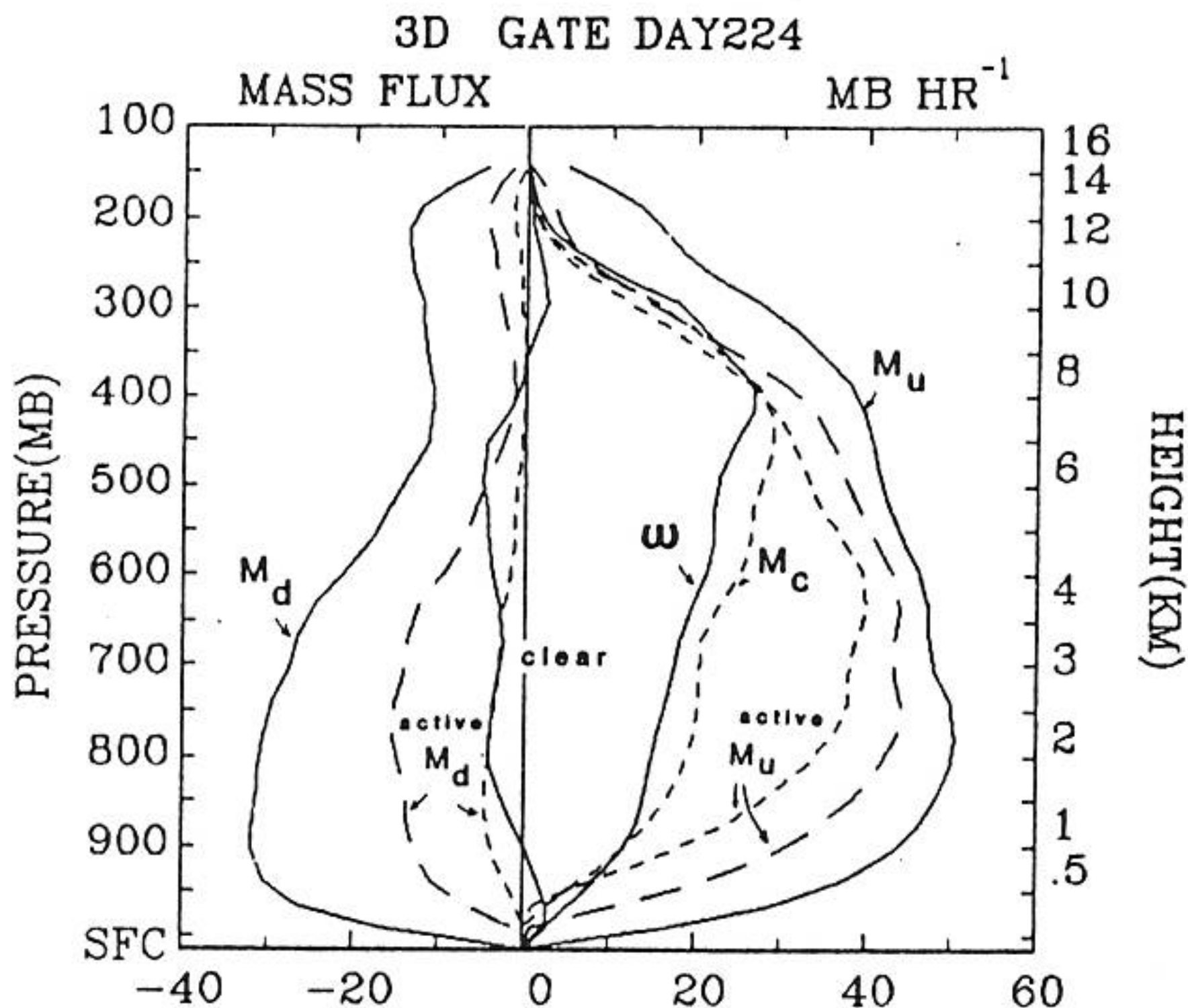
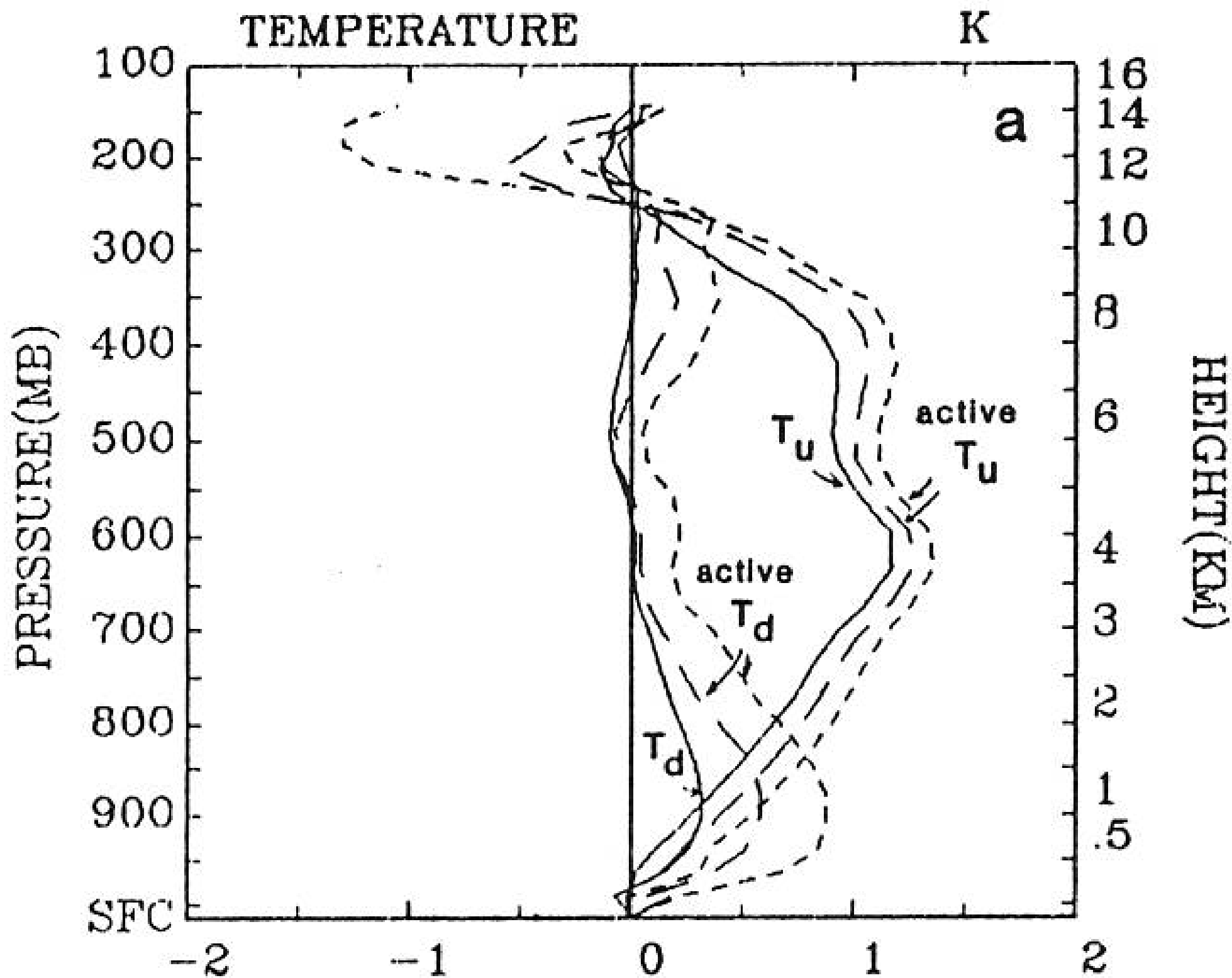


FIG. 3. Vertical profiles of the upward and downward mass fluxes inside all of the clouds and the vertical mass fluxes inside the active updrafts and downdrafts. M_u denotes upward mass flux inside clouds, M_d downward mass flux inside clouds. Total cloud mass flux M_c ($=M_u + M_d$). ω is the imposed large-scale lifting forcing.

3D GATE DAY224



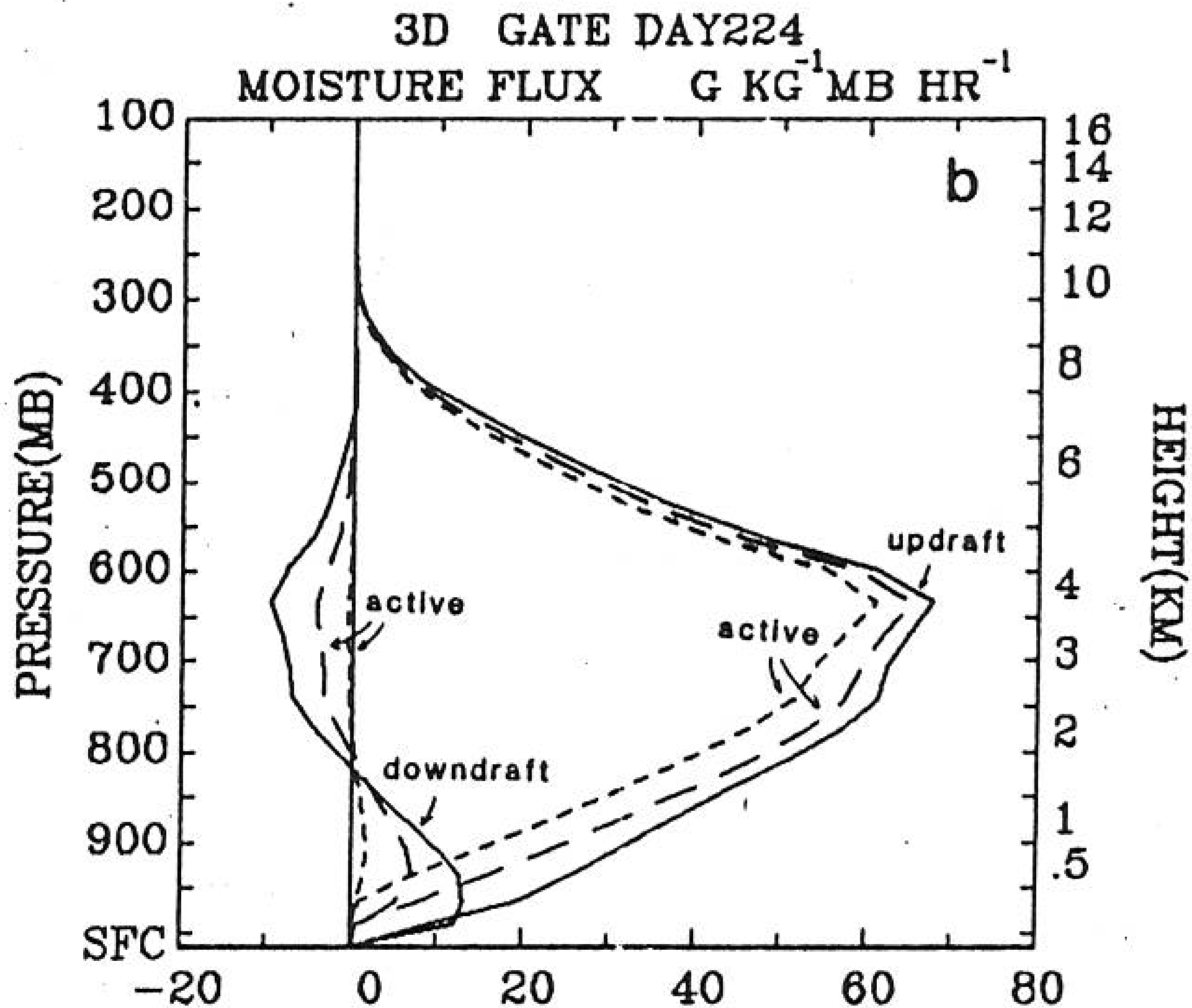
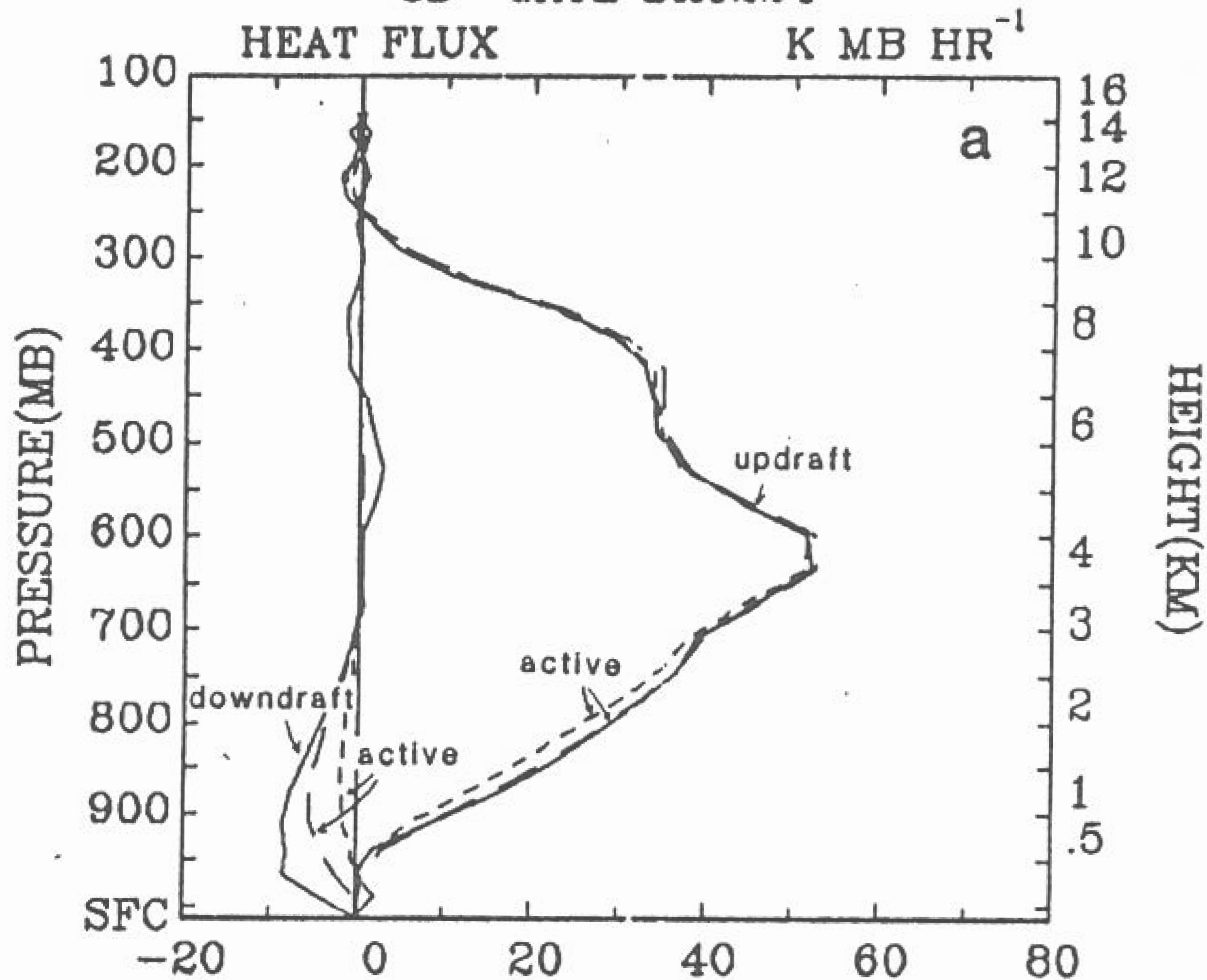


FIG. 5. As in Fig. 4 except for (a) sensible heat and (b) moisture fluxes inside cloud updraft and downdraft areas.

3D GATE DAY224



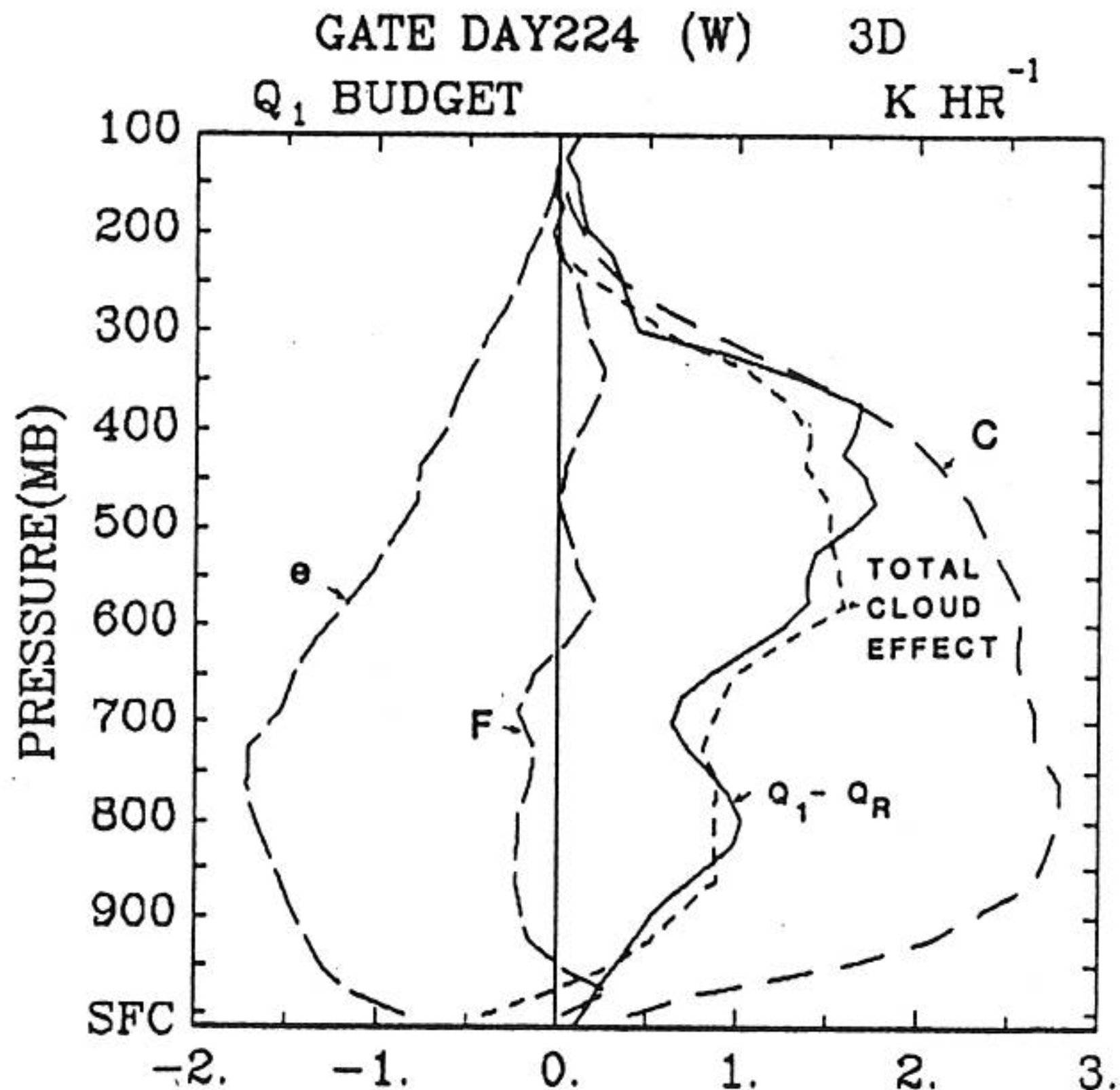


FIG. 9. The vertical profiles of the heating rate by condensation of moisture (C), evaporation of liquid water drops (e), net vertical flux of the sensible heat (F), the total heating rate by clouds and the heating rate estimated from large-scale observations, $Q_1 - Q_R$.

Fig. 2 : $\sigma \ll 1$ ($\sigma = \text{area of active updrafts}$)

Fig. 3 :
$$\begin{cases} M_c \approx W = \rho \bar{W} = M_c + \tilde{M} \\ M_c > \tilde{M} \end{cases}$$

so $\sigma W_c > (1-\sigma) |\tilde{W}| \approx |\tilde{W}|$

or $W_c > \frac{|\tilde{W}|}{\sigma} > |\tilde{W}|$

so $W_c \gg \tilde{W}$.

Fig-6 : $T_c - \tilde{T} \ll \tilde{T}$
 $q_c - \tilde{q} \leq \tilde{q}$

Fig. 5: Shows $\rho \overline{s'w'} \approx M_c (s_c - \bar{s})$.

Here, $\rho \overline{s'w'} = \rho \overline{s'w'}_{up} + \rho \overline{s'w'}_{down}$
where

$$\rho \overline{s'w'}_{up} = M_u (s_u - \bar{s})$$

$$\rho \overline{s'w'}_{down} = M_d (s_d - \bar{s})$$

u, d: up, down drafts in cloud; see Fig. 8.

Fig. 4: c, e ($g\ kg^{-1}\ hr^{-1}$)

Fig. 9: $Q_1 - Q_R$, components